Journal of Solid State Chemistry 184 (2011) 154–158

Contents lists available at ScienceDirect

Journal of Solid State Chemistry

journal homepage: www.elsevier.com/locate/jssc

Bismuth titanate pyrochlore microspheres: Directed synthesis and their visible light photocatalytic activity

Jungang Hou [a,*], Shuqiang Jiao [a], Hongmin Zhu [a], R.V. Kumar [b]

[a] School of Metallurgical and Ecological Engineering, University of Science and Technology Beijing, Beijing 100083, China
[b] Department of Materials Science and Metallurgy, University of Cambridge, Cambridge CB2 3QZ, United Kingdom

ARTICLE INFO

Article history:
Received 13 October 2010
Received in revised form
6 November 2010
Accepted 9 November 2010
Available online 18 November 2010

Keywords:
Bismuth titanate
Microspheres
Photocatalytic activity
RhB degradation

ABSTRACT

Bismuth titanates, $Bi_2Ti_2O_7$ (BIT), with well-defined spherical structures were synthesized by a facile hydrothermal process without the use of any surfactant or template. XRD and SEM studies have shown that spheres could be fabricated in high yields by simply manipulating the concentrations of hydroxide ions. In this case, hydroxide ions seem to play a pivotal role in controlling the formation of seeds and growth rates of the BIT particles. On the basis of structural analysis of samples obtained at different concentrations of OH^-, we also proposed a plausible mechanism to account for the formation of these distinctive morphologies under different conditions. The as-prepared BIT microspheres with good stability exhibited higher photocatalytic activities in the degradation of Rhodamine B (RhB) under visible light irradiation than that in commercial P25 TiO_2. Furthermore, the enhanced photocatalytic performance for RhB degradation was also investigated with assistance of a small amount of H_2O_2.

1. Introduction

Environmental problems, such as organic pollutants and toxic water pollutants, provide the impetus for the fundamental and applied research in the environmental area. Photocatalysis using solar energy is favorably expected to be an ideal "green" technology for sustainable development of human beings where an active photocatalytic material offers the potential for the elimination of toxic chemicals through its efficiency and broad applicability [1]. To date, TiO_2 is well-known as a stable, low cost, environmental friendly and highly efficient photocatalytic material [1–4] while its application is limited at the ultraviolet light region ($\lambda < 400$ nm). In order to achieve efficient utilization of visible light, the discovery of an active visible light-driven photocatalysts has attracted much attention. Recently, numerous oxides such as $NiO_x/In_{0.9}Ni_{0.1}TaO_4$, $SrTiO_3$, $NaTaO_3$, $BiVO_4$ and Bi_2WO_6, have been reported to show high activities [4–9].

In heterogeneous photocatalysis, the morphology of the catalyst plays a key role in catalytic activity [10–12]. Disperse spherical structures have attracted extensive attention in materials science, chemistry and biology as a result of their unique properties and their wide range of potential applications, which can be tuned by changing parameters such as diameter, chemical composition, bulk structure and crystallinity. In recent years, much progress have been made on the preparation of disperse inorganic nanospheres, such as Bi, Pb, Se, metal alloys, and their functional core-shell structures, carbon, magnetic ferrite and cuprous oxide [13–22]. Thus, appropriate routes to synthesize disperse spheres are required for a variety of applications including photocatalysis.

Bismuth titanates, a large family that includes several phases in the Bi–O–Ti system, are promising candidates for various technological applications [23–34]. $Bi_2Ti_2O_7$, belongs to a family of $A_2B_2O_7$ compounds with pyrochlore structure. Considering the potential applications of bismuth titanate crystals, many kinds of morphologies have been reported, such as nanowires, nanoparticles, nanotube, etc. [23–34]. Radosavljevic et al. reported a route that resulted in a Bi–O–Ti composition of the form $Bi_{1.74}Ti_2O_{6.25}$ [35]. Hector and Wiggin reported the synthesis and structural study of stoichiometric BTO along with some $Bi_4Ti_3O_{12}$ impurities using a co-precipitation method [36]. On the basis of the previous work on the preparation of bismuth titanate, we have introduced a low-temperature solution-phase route without the use of any surfactant and template to synthesize BIT spheres with controlled diameter and crystallinity. As stimulated by the promising applications, the synthesis of bismuth titanate spheres, is a subject of considerable research interest.

In this work, we report the synthesis and morphology of BIT spheres through a facile template-free hydrothermal process. There are two significant aspects of the work described in this paper. Firstly, the synthesis of shape-controlled BIT spheres has been prepared. Secondly, the disperse BIT microspheres associated optical properties and photocatalytic activities (using the degradation of Rhodamine B) under visible-light irradiation has been investigated and discussed.

* Corresponding author.
E-mail addresses: hjgwolf2004@163.com, lorinhjg@yahoo.com.cn (J. Hou).

0022-4596/$ - see front matter Crown Copyright © 2010 Published by Elsevier Inc. All rights reserved.
doi:10.1016/j.jssc.2010.11.017

2. Experimental section

2.1. Sample preparation

A surfactant-free and template-free solution-phase synthesized route to BIT spheres is described below. Bismuth nitrate and titanium isopropoxide were used as starting materials with the molar ratios of bismuth: titanium ions, 1:1. $Bi(NO_3)_3 \cdot 5H_2O$ and $Ti(OC_3H_7)_4$ were dissolved in 10 mL of deionized water under vigorous stirring and then mixed with a KOH (Aldrich, 99.9%) solution inside a stirred, closed vessel made of polypropylene. The concentration of the alkali solution was adjusted using KOH, which in effect served as a capping agent. Before being transferred to a 23 mL Teflon-lined autoclave, the solution mixture was prepared under an ultrasonic water bath for 30 min in order to avoid the premature formation of bismuth titanate nuclei induced by the concentration of KOH and kept at a filling ratio of 80% (v/v). The hydrothermal synthesis was conducted at 180 °C in an electric oven. After the reaction, BIT spheres were harvested by centrifugation and thorough washings with deionized water.

2.2. Characterization

The obtained products were characterized with field emission scanning electron microscopy (FESEM, JEOL, JSM-6340 F), X-ray diffraction (XRD) with Cu$K\alpha$ radiation ($\lambda = 1.5406$ Å) operated at a current of 40 mA and a voltage of 40 kV. The surface area of the BIT microspheres was measured by TriStar 3000-BET/BJH Surface Area. Then, the adsorption UV–vis spectrum of the centrifuged solution was recorded using a UV–vis spectrophotometer (Perkin Elmer Lambda 850).

2.3. Photocatalytic test

Photocatalytic activities of the photocatalysts were evaluated by the degradation of RhB under visible light irradiation using a 300 W Xe lamp ($\lambda > 420$ nm) as the light source. The reaction bath was placed in a sealed black box. The top of the box was opened and the cut-off filter was set on the window face of the reaction bath to ensure the desired irradiation conditions. In each experiment, 100 mg photocatalyst was added into 100 mL RhB aqueous solution (10^{-5} mol L^{-1}). Before illumination, the suspensions were magnetically stirred in the dark for 30 min to ensure the establishment of an adsorption–desorption equilibrium between the photocatalyst and RhB. At given time intervals, a 3 mL suspension was sampled and centrifuged to remove the photocatalyst particles.

3. Results and discussion

3.1. Crystal structure characterization

Fig. 1 showed the X-ray diffraction (XRD) patterns of BIT spheres from the synthesis method described above before photocatalytic reactions. All the peaks could be well-indexed to a pure cubic phase ($a = 20.67$ Å) of BIT, which are consistent with the literature [25]. No peaks of impurities were detected from this pattern. The strong and sharp peaks indicate that the as-obtained products are highly crystallized. Besides, the EDS analysis data of Table 1 (Supporting Information), the experimentally observed atomic ratios agreed with the initial compositions signifies that the BIT spheres without the incorporation of alkali metal cations are single phase. From the application point of view, the stability of a photocatalyst is important. In the case of BIT spheres, the crystal structure of the BIT spheres was very stable, as demonstrated by XRD spectra (Fig. 1) after the reaction with RhB.

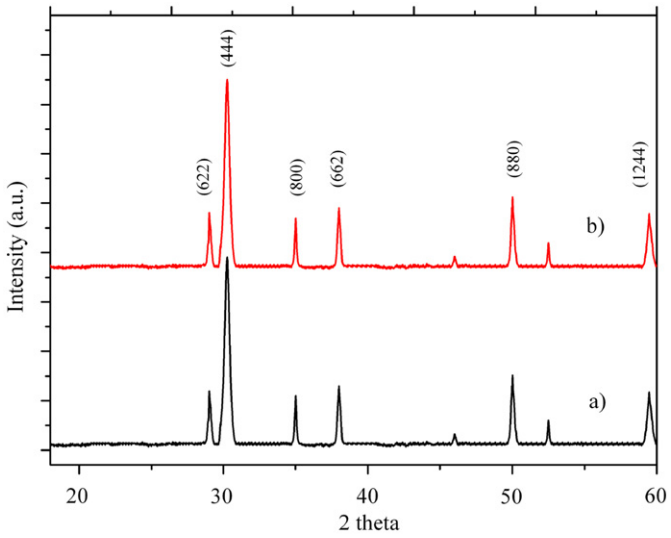

Fig. 1. XRD patterns of $Bi_2Ti_2O_7$ spheres before (a) and after (b) photodegradation.

3.2. Morphology analysis

The morphology of $Bi_2Ti_2O_7$ spheres prepared at 180 °C for 24 h was studied by SEM, as shown in Fig. 2. Under these conditions, the product is complete in morphology, implying that a high yield can be achieved in the reaction conditions through this facile surfactant-free solution-phase route. The influence of different OH^- concentrations on the morphology of bismuth titanate crystals was present. Using KOH with concentrations in the range from 3 to 10 M, all resulted in the formation of bismuth titanate spheres with nearly smooth surfaces. As we all know, the KOH concentration in the precursor solution has been found to be very important for the microstructure. It has been reported that the morphologies of $Bi_2Ti_2O_7$ spheres can be controlled by adjusting the OH^- concentration suggesting that OH^- ions can behave as a surfactant, obtaining a better understanding of the role of OH^- ions in the hydrothermal process [37].

Fig. 3 shows the relationship between the diameter of $Bi_2Ti_2O_7$ spheres and the OH^- concentration. As the OH^- concentration was increased, there was a monatomic increase in the diameter. The data points could be fitted using square equation $C \propto d^2$, where d is the average diameter and C is the total OH^- concentration. We could easily tune the average diameter of these spheres from 200 to 750 nm by varying the OH^- concentration in the range from 3 to 10 M. Thus, we believe that KOH behaves not only as a mineralizer but also as a surfactant in the hydrothermal process: the OH^- concentration can play a key role in the formation of the $Bi_2Ti_2O_7$ spheres.

On the basis of previous report about hierarchical $Bi_{0.5}Na_{0.5}TiO_3$ (BNT) micro/nanostructure and bismuth titanate microflowers and nanowires [33,34], the morphologies associated with the mechanism for the formation of BIT spheres prepared at different times are shown (see Fig. S1). At lower concentration of OH^- and for shorter reaction time, only particles were obtained, which are in agreement with our report [33]. When the reaction time is prolonged, the primary nanoparticles grow and aggregate, picking up freshly formed microparticles. Increasing the reaction time, the BIT microspheres are obtained. Besides, when the concentration of OH^- is further increased, the most plausible mechanism for the growth of the disperse BIT spheres is that nanoparticles nucleate, grow and

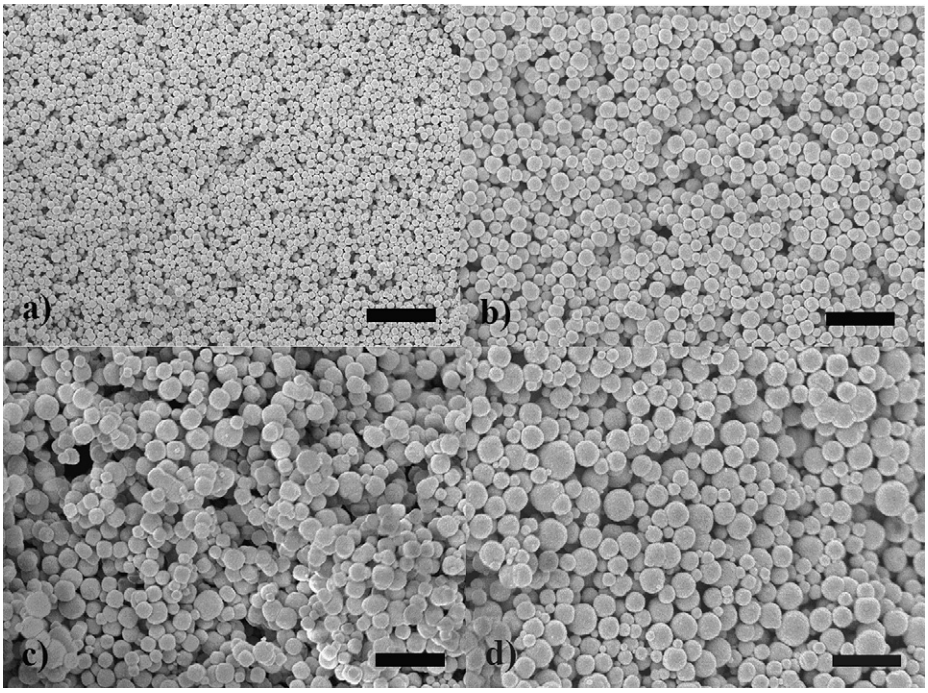

Fig. 2. SEM patterns of $Bi_2Ti_2O_7$ spheres with different concentrations of OH^-: (a) 3 M, (b) 5 M, (c) 8 M and (d) 10 M. Bar size=2.5 μm.

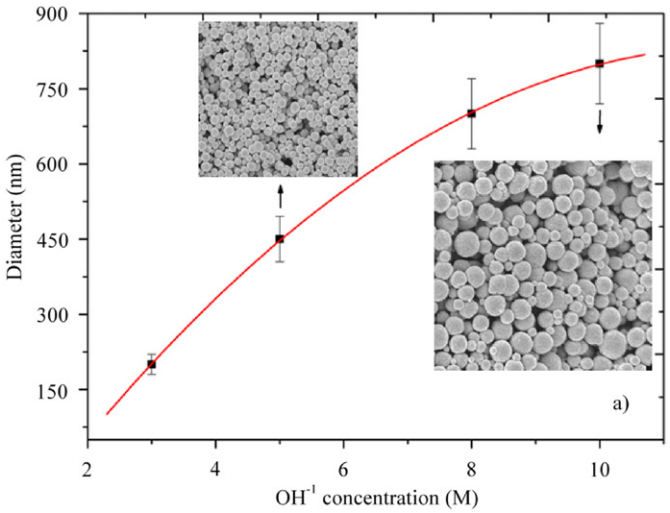

Fig. 3. Plot showing the relationship between the diameter of the $Bi_2Ti_2O_7$ spheres and concentration of OH^-.

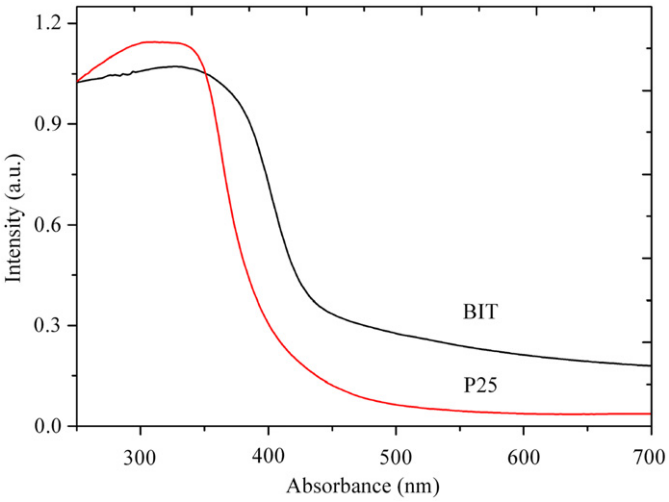

Fig. 4. UV absorption spectra of $Bi_2Ti_2O_7$ spheres and P25 TiO_2.

aggregate. On further increase of OH^- concentration, the nanoparticles on the spheres will dissolve and recrystallize. At very high concentration of OH^-, the formation of sheet-like particles is followed by ripening giving rise to the resulting structure of nanosheets growing out from the microspheres [33]. Thus, the pH value plays a pivotal role in controlling the formation of seeds and the growth rates to shape the $Bi_2Ti_2O_7$ particles.

3.3. UV–vis diffuse reflectance spectra

Fig. 4 shows the UV absorption spectra of the BIT spheres and P25 TiO_2. The band gap absorption edge of BIT spheres is determined to be 437 nm. For a crystalline semiconductor, the optical absorption near the band edge follows the equation [38,39].

$$\alpha h\upsilon = A(h\upsilon - E_g)^{n/2} \quad (1)$$

where α, v, E_g, and A are absorption coefficient, light frequency, band gap and a constant, respectively. According to the equation above, the value of n for $Bi_2Ti_2O_7$ spheres is 1. The band gap energy of $Bi_2Ti_2O_7$ is calculated to be 2.83 eV, which displays a marked red shift in the absorbance compared to P25 TiO_2 due to the contribution of 6s electrons from Bi^{3+} [25]. These experimental results for the band gap energy of $Bi_2Ti_2O_7$ are in agreement with the data reported by Yao and Hector [23,36], indicating that BIT spheres have potential ability for photocatalytic decomposition of organic contaminants under visible light irradiation.

3.4. Photodegradation of RhB

The photocatalytic activities of the as-prepared BIT spheres were evaluated by the degradation of RhB solution. Fig. 5 shows the temporal evolution of the absorption spectrum of RhB solution (10^{-5} mol L^{-1}) in the presence of 100 mg of BIT spheres (3 M) in

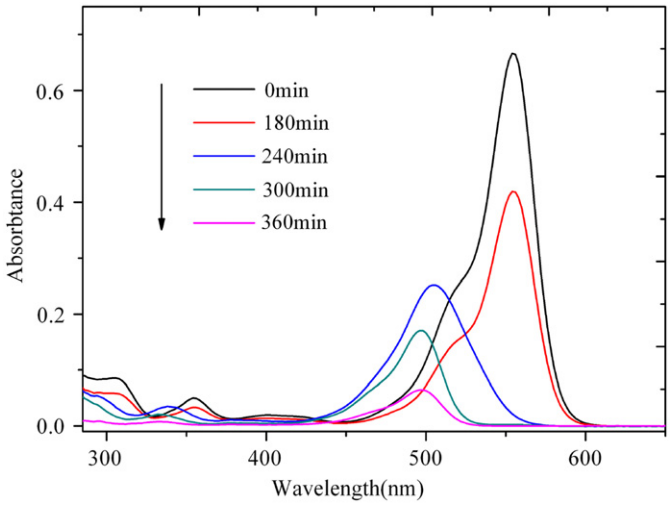

Fig. 5. Temporal evolution of the absorption spectrum of RhB solution (1×10^{-5} M) in the presence of 100 mg of $Bi_2Ti_2O_7$ spheres (3 M) in 100 mL solution under visible light irradiation.

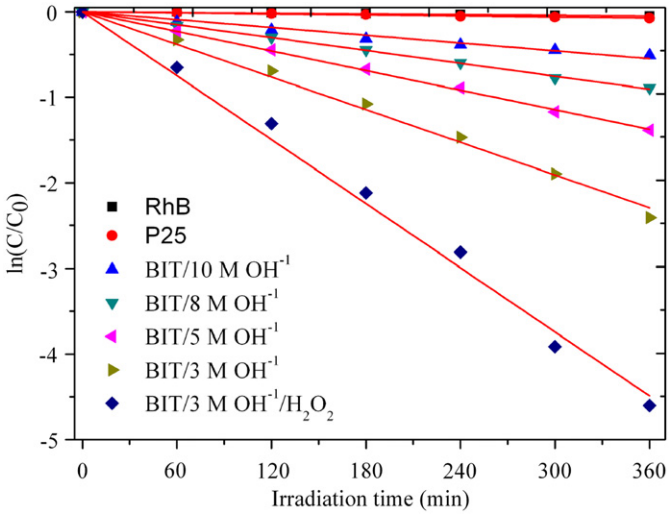

Fig. 7. Kinetic linear curves of RhB photocatalytic degradation with $Bi_2Ti_2O_7$ and P25.

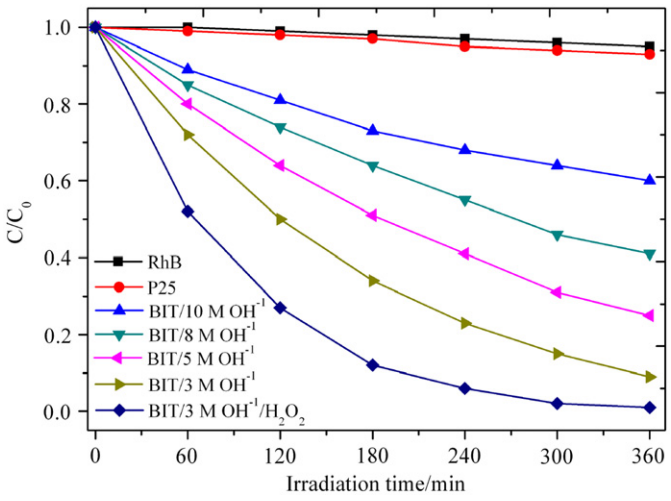

Fig. 6. RhB normalization concentration (C_0: 1×10^{-5} M) in the solution (100 mL) with the $Bi_2Ti_2O_7$ spheres (100 mg) versus the exposure time under visible light irradiation.

100 mL solution under visible light irradiation. The absorption peak corresponding to the RhB molecules at 553 nm rapidly decreased in intensity with exposure time. Absorption spectra reveal no evidence of the existence of new intermediates or products formed in the visible region. The color of the suspension changed the light gradually and disappeared ultimately. However, under visible light irradiation, the absorbance of the suspension decreases with a concomitant wavelength shift of the band to shorter wavelength, and the new band around 500 nm occurs. The color of the suspension changes from an initial red color to a final achromatic color. Almost complete degradation of RhB was achieved when exposed to visible light irradiation for 360 min. The peak blue shift could be ascribed to *N*-de-ethylation of RhB to rhodamine (see Fig. S2) [40]. Fig. 6 shows the degradation rates of RhB using the BIT spheres with varying diameters. It shows that there was a negligible change in the degradation of RhB arising only from the slow evaporation for the RhB solution without any catalyst. However, with the decrease in diameters when hydroxyl concentration was decreased from 10 to 3 M, the degradation rate of RhB increases from 30% to 91% for $Bi_2Ti_2O_7$ spheres after 360 min. In comparison, the photocatalytic degradation rate of RhB over P25 was only 7%. Thus, the addition of $Bi_2Ti_2O_7$ catalysts leads to the obvious degradation of RhB, and the photocatalytic activity depends on the diameter of spheres, which results from separation and stabilization of photo-electrons and photo-generated holes [23,25]. Moreover, when 0.25 mL H_2O_2 (30 wt%) was introduced into the photoreaction suspension, the BIT/H_2O_2 (3 M OH^-) system could degrade almost 100% of RhB after 360 min, which suggests a remarkable enhancement in photocatalytic activity. However, as the BET surface area of the samples increases, there is a resulting increase in adsorption percentages of RhB molecules. The higher BET surface area (15 m^2/g) of the BIT spheres provides more active sites for photocatalytic reaction, resulting in the superior photocatalytic activity.

Furthermore, the kinetic linear simulation curves of RhB photocatalytic degradation with BIT and P25 are shown in Fig. 7. It is clear that the curve with irradiation time as abscissa and $\ln(C/C_0)$ as the vertical ordinate is close to a linear curve, which indicates the photocatalytic degradation of RhB using BIT spheres follows first-order reaction kinetics. The values of k for RhB, P25 and BIT with various concentrations of 10, 8, 5 and 3 M are 0.00013, 0.0002, 0.00152, 0.0025, 0.0038 and 0.0064 min^{-1}, respectively, indicating higher photocatalytic performance of BIT spheres than that of commercial P25 TiO_2. After the addition of 0.25 mL H_2O_2, the constant rate reaches 0.0125 min^{-1}, indicating the better photocatalytic performance of the BIT/H_2O_2 (3 M OH^-) system. It is worth pointing out that the stability of a given photocatalyst during photoreaction is a crucial factor for the practical applications. The stability tests were investigated by carrying out recycling reactions four times for the photodegradation of RhB over BIT photocatalyst under visible light irradiation, and the results are shown in Fig. 8. No decrease in catalytic activity was observed in the recycling reactions. Combined with the XRD patterns, all evidences demonstrate that the BIT spheres have good stability.

Based on the above observations, a possible photocatalytic mechanism of BIT is proposed and a schematic diagram is shown in Fig. 9. In this photodegradation process, the photoexcited electrons can be transferred to the conduction band (CB) from the valence band (VB), and while the holes form in the VB when BIT spheres is irradiated by light. Then the photoexcited holes in the VB can form ·OH (hydroxyl radical) that can oxidize the organic pollutants and the electrons in the CB participate in a reduction process. The higher photocatalytic activity of BIT over TiO_2 was

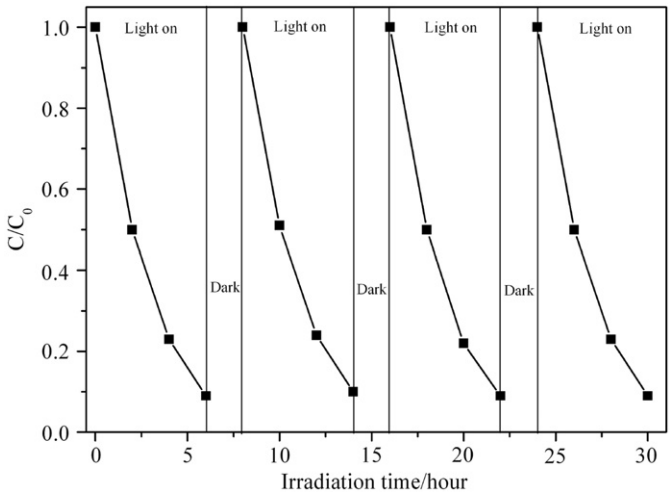

Fig. 8. Stability evaluation for $Bi_2Ti_2O_7$ spheres: four reaction cycles for photodegradation of RhB under visible light irradiation.

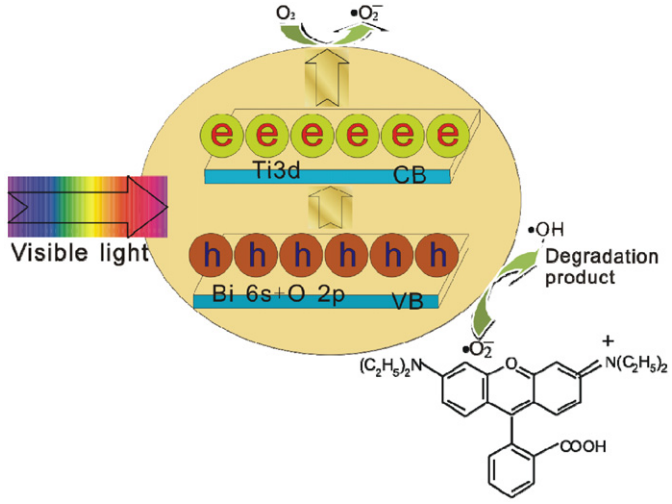

Fig. 9. Schematic diagram of photocatalytic mechanism for $Bi_2Ti_2O_7$ spheres.

attributed to be suitable band gap and stable e–h pair formation in the valence band formed by the hybrid orbitals of Bi 6*s* and O 2*p* and the conduction band of Ti 3*d* [41,42].

4. Conclusion

Bismuth titanates with well-defined spherical structures were synthesized by a facile hydrothermal process without the use of any surfactant or template. XRD and SEM studies have shown that spheres could be fabricated in high yields by simply manipulating the concentration of hydroxide ions. In this case, hydroxide ions seem to play a pivotal role in controlling the formation of seeds and the growth rates of the BIT particles. Based on the structural analysis of samples obtained at different concentration of OH^-, we also proposed a plausible mechanism to account for the formation of these distinctive morphologies under different conditions. Most importantly, the BIT spheres with good stability exhibited higher photocatalytic performance in the degradation of RhB solution under visible light irradiation than commercial P25 TiO_2. Furthermore, the higher performance of small BIT spheres with the assistance of a small amount of H_2O_2 for RhB degradation indicates that BIT spheres is a promising candidate as a visible-light photocatalyst.

Acknowledgments

This work was supported by EPSRC, PCME Ltd., National Basic Research Program of China (973 Program, Grant no. 2007CB613301).

Appendix A. Supplementary data

Supplementary data associated with this article can be found in the online version at doi:10.1016/j.jssc.2010.11.017.

References

[1] M. Hoffmann, S. Martin, W. Choi, D. Bahnemann, Chem. Rev. 95 (1995) 69–96.
[2] H. Zhu, Y. Lan, X. Gao, S. Ringer, Z. Zheng, D. Song, J. Zhao, J. Am. Chem. Soc. 127 (2005) 6730–6736.
[3] Y. Ohko, D. Tryk, K. Hashimoto, A. Fujishima, J. Phys. Chem. B 102 (1998) 2699–2704.
[4] M. Karkmaz, E. Puzenat, C. Guillard, J. Herrmann, Appl. Catal. B: Environ. 51 (2004) 183–194.
[5] Z. Zou, J. Ye, K. Sayama, H. Arakawa, Nature 414 (2001) 625–627.
[6] K. Domen, A. Kudo, T. Onishi, J. Catal. 102 (1986) 92–98.
[7] H. Kato, A. Kudo, Chem. Phys. Lett. 295 (1998) 487–492.
[8] J. Yu, A. Kudo, Adv. Funct. Mater. 16 (2006) 2163–2169.
[9] H. Fu, S. Zhang, T. Xu, Y. Zhu, J. Chen, Environ. Sci. Technol. 42 (2008) 2085–2091.
[10] F. Lu, W.P. Cai, Y. Zhang, Adv. Funct. Mater. 18 (2008) 1047–1056.
[11] S. Xiong, B. Xi, C. Wang, D. Xu, X. Feng, Z. Zhu, Y. Qian, Adv. Funct. Mater. 17 (2007) 2728–2738.
[12] L. Zhang, W. Wang, L. Zhou, H. Xu, Small 3 (2007) 1618–1625.
[13] X. Jiang, T. Herricks, Y. Xia, Adv. Mater. 15 (2003) 1205–1209.
[14] U. Jeong, Y. Xia, Adv. Mater. 17 (2005) 102–106.
[15] Y. Wang, L. Cai, Y. Xia, Adv. Mater. 17 (2005) 473–477.
[16] Y. Wang, Y. Xia, Nano Lett. 4 (2004) 2047–2050.
[17] Q. Peng, Y. Dong, Y. Li, Angew. Chem. Int. Ed. 42 (2003) 3027–3030.
[18] X. Sun, Y. Li, Angew. Chem. Int. Ed. 43 (2004) 597–601.
[19] X. Sun, Y. Li, Angew. Chem. Int. Ed. 43 (2004) 3827–3831.
[20] H. Deng, X.L. Li, Q. Peng, X. Wang, J. Chen, Y. Li, Angew. Chem. Int. Ed. 44 (2005) 2782–2785.
[21] X. Li, T. Lou, X. Sun, Y. Li, Inorg. Chem. 43 (2004) 5442–5449.
[22] J. Wang, X. Wang, Q. Peng, Y. Li, Inorg. Chem. 43 (2004) 7552–7556.
[23] W.F. Yao, H. Wang, X.H. Xu, J.T. Zhou, X.N. Wang, Y. Zhang, S.X. Shang, Appl. Catal. A: Gen. 259 (2004) 29–33.
[24] J.G. Hou, Y.F. Qu, D. Krsmanovic, C. Ducati, D. Eder, R.V. Kumar, Chem. Commun. 26 (2009) 3937–3939.
[25] S. Murugesan, V. Subramanian, Chem. Commun. (2009) 5109–5111.
[26] J.G. Hou, Y.F. Qu, D. Krsmanovic, R.V. Kumar, J. Nanopart. Res. 12 (2010) 1797–1805.
[27] J. Zhou, Z. Zou, A. Ray, X. Zhao, Ind. Eng. Chem. Res. 46 (2007) 745–749.
[28] J.G. Hou, R.V. Kumar, Y.F. Qu, D. Krsmanovic, J. Nanopart. Res. 12 (2010) 563–569.
[29] S. Xu, W. Shangguan, J. Yuan, J. Shi, M. Chen, Mater. Sci. Eng. B 137 (2007) 108–111.
[30] V. Skorikov, I. Zakharov, V. Volkov, E. Spirin, V. Umrikhim, Inorg. Mater. 37 (2001) 1149–1154.
[31] L. Pintilie, I. Pintile, M. Alexe, J. Eur. Ceram. Soc. 19 (1999) 1473–1476.
[32] J.G. Hou, Y.F. Qu, D. Krsmanovic, R.V. Kumar, Scripta Mater. 61 (2009) 664–667.
[33] J.G. Hou, Y.F. Qu, D. Krsmanovic, C. Ducati, D. Eder, R.V. Kumar, J. Mater. Chem. 20 (2010) 2418–2423.
[34] J. Li, G. Wang, H. Wang, C. Tang, Y. Wang, C. Liang, W. Cai, L. Zhang, J. Mater. Chem. 19 (2009) 2253–2258.
[35] I. Radosavljevic, J.S.O. Evans, A.W. Sleight, J. Solid State Chem. 136 (1998) 63–66.
[36] A. Hector, S. Wiggin, J. Solid State Chem. 177 (2004) 139–145.
[37] J. Han, Y. Huang, X. Wu, C. Wu, W. Wei, B. Peng, W. Huang, J. Goodenough, Adv. Mater. 18 (2006) 2145–2148.
[38] M.A. Butler, J. Appl. Phys. 48 (1977) 1914–1920.
[39] J. Tang, Z. Zou, J. Ye, J. Phys. Chem. B 107 (2003) 14265–14269.
[40] T. Wu, G. Liu, J. Zhao, J. Phys. Chem. C 102 (1998) 5845–5851.
[41] W. Wei, Y. Dai, B.B. Huang, J. Phys. Chem. C 113 (2009) 5658–5663.
[42] H.F. Cheng, B.B. Huang, Y. Dai, X.Y. Qin, X.Y. Zhang, J. Solid State Chem. 182 (2009) 2274–2278.